Eur. Phys. J. B **56**, 83–91 (2007)
DOI: 10.1140/epjb/e2007-00094-6

THE EUROPEAN PHYSICAL JOURNAL B

Josephson current through a ferromagnetic semiconductor/semiconductor/ferromagnetic semiconductor structure

Y.C. Tao[a]

Department of Physics, Nanjing Normal University, Nanjing 210097, P.R. China

Received 10 October 2006 / Received in final form 26 January 2007
Published online 12 April 2007 – © EDP Sciences, Società Italiana di Fisica, Springer-Verlag 2007

Abstract. We theoretically calculate the Josephson current for two superconductor/ferromagnetic semiconductor (SC/FS) bilayers separated by a semiconductor (SM) layer. It is found that the critical Josephson current I_C in the junction is strongly determined by not only the relative orientations of the effective exchange field $\mathbf{h}$ of the two bilayers and scattering potential strengths at the interfaces but also the kinds of holes (the heavy or light) in the two FS layers. Furthermore, a robust approach to measuring the spin polarization P for the heavy and light holes is presented.

PACS. 74.50.+r Tunneling phenomena; point contacts, weak links, Josephson effects – 74.45.+c Proximity effects; Andreev effect; SN and SNS junctions – 75.50.Pp Magnetic semiconductors

1 Introduction

Information processing in electronic devices is on the basis of control of charge flow in semiconductor material, however nonvolatile information storage exploits ferromagnetism, spontaneous alignment of the spins of many electrons. Spintronics [1–5] aims to achieve a merger of these technologies, arousing interest in new ferromagntic semiconductor (FS) such as GaMnAs. A fundamental understanding of $Ga_{1-x}Mn_xAs$ is very relevant in this context since this is a *canonical* FS that remains the most thoroughly studied of all such materials [6], which makes it possible to combine the information processing and data storage in one material. The origin of ferromagnetism in the FS can be explained by applying a picture in which uniform itinerant carrier spin mediates a long-range ferromagnetic order between the ions Mn^{+2} with spin $s = 5/2$ [7–9]. Recent experiments demonstrate that the Curie temperature (T_C) of this material can be as high as 150 K [10], showing promise for possible technological relevance. The large tunneling magnetoresistance observed in magnetic tunnel junctions derived from this material implies that the spin polarization (P) may be large even for small Mn concentrations [11–13].

On the other hand, current can flow without dissipation through a thin insulating layer or weak link separating two superconductors (SC). A phase difference $\Delta\theta$ between the SCs appears due to the quantum character of the superflow. The current-phase relationship of the link is periodic function of $\Delta\theta$. For a tunnel barrier, as first found by Josephson [14], it is given by $I = I_C \sin(\Delta\theta)$ with I_C the critical current, where I_C can change sign when the SCs are coupled by a thin ferromagnet (FM) layer [15–29]. Referring to the Josphson current-phase relationship, this change corresponds to a π-phase shift of $\Delta\theta$. Thus Josephson junctions presenting a negative coupling are usually called π junctions. The critical current I_C decreases with increasing exchange field $\mathbf{h}$ in the FM layer, changes sign, and decays to zero while undergoing some oscillations. The superconducting properties are not so strongly reduced if the magnetization (i.e., the effective exchange field $\mathbf{h}$) is not homogeneous. Recently, Bergeret et al. [19] found that in the SC/FM/I/FM/SC junction with I an insulator, the critical current I_C strongly depends on the relative orientations of the effective exchange field $\mathbf{h}$ of the two bilayers.

In this work, we theoretically calculate the Josephson current of a SC/FS/semiconductor(SM)/FS/SC junction. It is found that the critical Josephson current I_C in the junction strongly depends on not only the relative orientations of the effective exchange field $\mathbf{h}$ of the two bilayers but also the kinds of holes (the heavy or light) in the FS and scattering potential strengths Z at the interfaces. In addition, a robust approach to measuring P for the heavy and light holes is presented. The study of the junction can provide new opportunities for the research of the SC

[a] e-mail: taoyongchun@njnu.edu.cn

and FS systems, which could not only be used for reliable spectroscopy of Josephson current and bring about promising interest for the further enhancement of the efficiency in magnetic sensors and memories but also be helpful to have an insight into the physical properties of the heavy and light holes in the FS.

2 Model and theory

Let us consider a junction which consists of two the same SC/FS bilayers with the FS GaMnAs layer of thickness b separated by a SM GaAs layer of thickness a. All the layers are assumed to be the x-y plane and stacked along the z-direction. For either the left and right FS/SC interfaces or SM/FS interfaces, it is well-recognized that the semiconducting interfaces are responsible for asymmetry in the current-voltage characteristics, related to the presence of space-charge regions (Schottky potential barrier) described by asymmetrical potential energy profiles [30], and the width of the potential barrier is proportional to $V^{\frac{1}{2}}$ with V the bias voltage. In this work, only the direct Josephson current is studied, which means that V is zero, therefore, the interfaces can be approximately described by four δ-type barrier potentials $V(x) = U\delta[z \pm (b + a/2)]$ and $V'(x) = U'\delta(z \pm a/2)$, respectively, as in references [12,25] and assumed to be symmetrical due to the same SCs and the same FS's, where U and U' depend on the product of the barrier height and width.

A free-hole model is applied to the FS GaMnAs with Γ the difference between the tops of the majority (M) and minority (m) valence subbands at the spins parallel and antiparallel to the local magnetization, respectively. Here, the valence subbands comprise heavy and light holes. The hole Hamiltonian in the FS is simply given by

$$H_{FS}(\mathbf{r}) = H_0(\mathbf{r}) - \mathbf{h}(\mathbf{r}) \cdot \sigma. \tag{1}$$

Here $H_0(\mathbf{r}) = -\hbar^2\nabla_{\mathbf{r}}/2m_p + V(\mathbf{r})$ is the kinetic energy with m_p the mass of a hole plus the usual static potential, which is also the hole Hamiltonian of the SM GaAs, $\mathbf{h}(\mathbf{r})$ is the effective exchange field with the magnitude $h(\mathbf{r})$ equal to $\Gamma/2$, and σ the conventional Pauli spin operator. At finite temperatures, the spin splitting energy $\Gamma(T)$ different for different kind of holes, is given by $\Gamma(T) = J_{pd}\langle S^z\rangle$, where J_{pd} refers to the $p-d$ exchange coupling strength between itinerant holes and Mn^{2+} ion impurity spins connected with the densities of Mn impurity and heavy or light holes, and $\langle S^z\rangle$ means the thermal average of the impurity Mn ion spins. In the F alignment, $\mathbf{h}(-b-a/2 \leq z \leq -a/2) = \mathbf{h}(a/2 \leq z \leq b + a/2)$, while in the A alignment, $\mathbf{h}(-b-a/2 \leq z \leq -a/2) = -\mathbf{h}(a/2 \leq z \leq b+a/2)$.

The SC is assumed s-wave pairing and described by a BCS-like Hamiltonian, in which the excitation energy is $\zeta_k = \sqrt{\epsilon_k^2 + \Delta^2}$ with $\epsilon_k = \hbar^2k^2/2m_e - E_F$ the one-electron energy relative to E_F and Δ the order parameter taken as in the form $\Delta(\mathbf{r}) = \Delta[\Theta(z - b - a/2) + \Theta(-z - b - a/2)]$. The order parameter is determined by the self-consistent equation

$$\ln\left(\frac{\Delta_0}{\Delta}\right) = \int_0^{\hbar\omega_D} \frac{d\epsilon_k}{\zeta_k} \frac{2}{1 + e^{\beta\zeta_k}}, \tag{2}$$

where ω_D refers to Debye frequency and Δ_0 denotes energy gap at zero temperature. The BCS coherence factors are given by $u_k^2 = (1 + \epsilon_k/\zeta_k)/2$ and $v_k^2 = (1 - \epsilon_k/\zeta_k)/2$.

The quasiparticle wave function is described by the following Bogoliubov-de Gennes (BDG) equation

$$\begin{bmatrix} H_0^{SC}(\mathbf{r}) - \eta_\sigma h(\mathbf{r}) & \Delta(\mathbf{r}) \\ \Delta^*(\mathbf{r}) & -H_0^{SC}(\mathbf{r}) + \eta_{\overline{\sigma}} h(\mathbf{r}) \end{bmatrix} \begin{bmatrix} u_\sigma(\mathbf{r}) \\ v_{\overline{\sigma}}(\mathbf{r}) \end{bmatrix} = E \begin{bmatrix} u_\sigma(\mathbf{r}) \\ v_{\overline{\sigma}}(\mathbf{r}) \end{bmatrix}, \tag{3}$$

where $H_0^{SC}(\mathbf{r})$ has the same expression as $H_0(\mathbf{r})$ except for the effective mass replaced by m_e, E is the quasiparticle energy relative to the Fermi energy E_F, $\overline{\sigma}$ is the spin opposite to σ with $\uparrow$ and $\downarrow$, $\eta_\sigma = 1$ for $\sigma =\uparrow$, and $\eta_\sigma = -1$ for $\sigma =\downarrow$. In equation (3), the spin-flip process has been neglected in the SC near interfaces, as a result, the spin-dependent (four-component) BDG equation may be coupled into two sets of two-component equations: $(u_\sigma, v_{\overline{\sigma}})$ describing the spin-σ electronlike quasiparticle (ELQ) and spin-$\overline{\sigma}$ holelike quasiparticle (HLQ).

For the injection of an ELQ from the left SC with Andreev reflection as a HLQ (a) and normal reflection (b), the wave functions are given by

$$\psi_L^{SC}(z) = [e^{ik^+z} + be^{-ik^+z}] \begin{pmatrix} ue^{i\phi_L/2} \\ ve^{-i\phi_L/2} \end{pmatrix} + ae^{ik^-z} \begin{pmatrix} ve^{i\phi_L/2} \\ ue^{-i\phi_L/2} \end{pmatrix}, \tag{4}$$

for $z \leq -b - a/2$,

$$\psi_R^{SC}(z) = ce^{ik^+z} \begin{pmatrix} ue^{i\phi_R/2} \\ ve^{-i\phi_R/2} \end{pmatrix} + de^{-ik^-z} \begin{pmatrix} ve^{i\phi_R/2} \\ ue^{-i\phi_R/2} \end{pmatrix}, \tag{5}$$

for $z \geq a/2 + b$, and

$$\psi_\gamma(z) = [c_{\gamma1}e^{iq^+_{\gamma\sigma}z} + c_{\gamma2}e^{-iq^+_{\gamma\sigma}z}] \begin{pmatrix} 1 \\ 0 \end{pmatrix} + [c_{\gamma3}e^{iq^-_{\gamma\overline{\sigma}}z} + c_{\gamma4}e^{-iq^-_{\gamma\overline{\sigma}}z}] \begin{pmatrix} 0 \\ 1 \end{pmatrix} \tag{6}$$

with $\gamma = 1$ for $-b - a/2 \leq z \leq -a/2$, $\gamma = 2$ for $-a/2 \leq z \leq a/2$, and $\gamma = 3$ for $a/2 \leq z \leq a/2 + b$, where $q^\pm_{\gamma\sigma} = \sqrt{(2m_p/\hbar^2)(E_F \pm E + \eta_\sigma h) - \mathbf{k}_\parallel^2}$ with $h \neq 0$ for $\gamma = 1$ or 3 and $h = 0$ for $\gamma = 2$, $k^\pm = \sqrt{(2m_e/\hbar^2)(E_F \pm \Omega) - \mathbf{k}_\parallel^2}$, $u = \sqrt{(1 + \Omega/E)/2}$, and $v = \sqrt{(1 - \Omega/E)/2}$ with $\Omega = \sqrt{E^2 - \Delta^2}$ and the parallel component of the wave vector

$\mathbf{k}_\parallel$ which is conserved. In the following, we use $q'^{\pm}$ and $q_\sigma^{L(R)\pm}$ to stand for the wave vectors with $\gamma = 2$ in the SM and $\gamma = 1\,(3)$ in the left (right) FS. In equations (4–6), all coefficients will be determined by the usual matching conditions of the wave functions.

From equations (4–6), we obtain the transmission and reflection coefficients. As the analytical results for these coefficients are tedious, we only give the expressions for a in the Appendix. In the derivation, $Z = 2m_eU/(\hbar^2 k_F^{SC})$ and $Z' = 2m_eU'/(\hbar^2 k_F^{SC})$ are introduced to describe the interface scattering strengths at the interfaces which are phenomenological parameters that take into the effects of the physical barrier (potential scattering as well as that of the band structure mismatch), χ refers to the ratio of the masses m_p and m_e, $\phi = \phi_L - \phi_R$, $|\mathbf{k}_\parallel| = k_F^{SC}\sin\theta$, where the corresponding Fermi vector in the SC is $k_F^{SC} = \sqrt{2m_eE_F}/\hbar$. Analogously, one can easily obtain the Andreev reflection (a') as an ELQ for the injection of a HLQ into the left FS from the left SC.

Having obtained the coefficients a and a', the dc Josephson current can be expressed in terms of the Andreev reflections amplitudes by using the temperature Green's function formalism [31]

$$I = \frac{e\Delta}{2\hbar}\sum_{\sigma,\mathbf{k}_\parallel} k_BT\sum_{\omega_n}\frac{1}{2\Omega_n}(k_n^+ + k_n^-)\left(\frac{a_n}{k_n^+} - \frac{a_n'}{k_n^-}\right), \quad (7)$$

where k_n^+, k_n^-, a_n, and a_n' are obtained from k^+, k^-, a, and a' by the analytic continuation $E \to i\omega_n$, the Matsubara frequencies are $\omega_n = \pi k_BT(2n+1)$ with $n = 0, \pm 1, \pm 2...$, and $\Omega_n = \sqrt{\omega_n^2 + \Delta^2}$. For the same E, σ, and θ in the approximation with $\Omega/E_F \ll 1$ and $E/E_F \ll 1$, the amplitudes of two Andreev reflections $a(\phi)$ and $a'(\phi)$ are simply connected by $a'(\phi) = a(-\phi)$.

3 Calculation and results

Performing integration over $\mathbf{k}_\parallel$, we can obtain

$$I = \frac{2\pi k_BT\Delta}{eRk_F^{SC}}\int_0^{\pi/2} d\theta \sin\theta\cos\theta \sum_{\omega_n,\sigma}[a_n(\phi) - a_n(-\phi)], \quad (8)$$

where $R = 2\pi^2\hbar/Se^2(k_F^{SC})^2$ with S the area of junction. To model the subband spin splitting in the FS and relative degree of P, we define the parameter $P \equiv \Gamma/E_F$. According to equation (8), we can calculate the Josephson currents in the F and A alignments.

Figure 1 shows the dependences of the normalized critical current I_C on P' at different scattering potential strengths Z and Z' in the F alignment for the heavy and light holes, where P' is define as $P' \equiv \Gamma/\Delta_0 = PE_F/\Delta_0$ [19]. The parameters $E_F = 100.0$ meV, $m_e = 1.0$, $m_p = 0.45m_e$ for the heavy hole and $0.08m_e$ for the light hole in the FS and SM [11,32], $\Delta_0 = 1.4$ meV, $k_BT = 0.05\Delta_0$, $a = 40/k_F^{SC}$, and $b = 20/k_F^{SC}$. It is found that the critical Josephson current I_C for the heavy holes, at $Z = 0$ and $Z' = 0$, increases with P', whereas, for the light, decreases. For Z or Z' unequal to zero, the situations are very different. When $Z' = 0$, for the heavy hole, I_C always increases with P' for the small Z and decreases for the big Z, while when $Z = 0$, for some Z', I_C increases with P', and for other Z', decreases. For the light hole, the critical Josephson currents I_C are found, at $Z' = 0$, to decrease all the time with P' in spite of Z, however at $Z = 0$, there exist the same features of I_C with variation of P' as those for heavy holes.

In Figure 2, the P' dependences of Josephson critical current I_C for the heavy and light holes in the A alignment are plotted at different Z and Z'. It is found that there are some features similar to those in Figure 1, for example, when $Z\,(Z') = 0$, for the heavy hole, I_C increases at some Z' with P' and decreases at other Z'. Simultaneously, it is shown that some behaviors and values of the critical Josephson currents I_C with increasing P' are remarkably different from those in Figure 1, which obviously originates from the existence of spin splitting energy in the FS's and resultant different mismatches in the Fermi vectors between the FS and SC for the F and A alignments. The critical Josephson current in the A alignment I_C for the heavy holes, at $Z = 0$ and $Z' = 0$, decreases with P', while for the light, basically has no change. In addition, I_C in the A alignment, at $Z\,(Z') = 0$, always increases with P' for the light holes no matter how $Z'(Z)$ varies.

In Figure 3 is illustrated the Z (Z') dependence of Josephson critical current I_C for different Z' (Z) in the F alignment for the heavy and light holes. Here $P' = 0.9$, and the other parameters are the same as in Figure 1. The critical Josephson currents I_C for the heavy holes, is found to show oscillations with the increase of $Z\,(Z')$, finally reduce to zero and there exist two peaks, however, at $Z' = 0$, firstly increase with increasing Z, whereas at $Z = 0$, firstly decreases and then increases with the enhancement of Z'. For the light hole, the critical Josephson currents I_C is also found to show oscillations with the increase of $Z\,(Z')$. In the meantime, one can notice that for $Z' = 0$, I_C firstly decreases with the enhancement of Z', while for $Z = 0$, I_C firstly increase and then decrease with enhancing of Z'. At Z and Z' unequal to zero, the varied behaviors of I_C with Z' and Z are also very similar, and I_C basically decreases, then increases, and lastly decreases to zero with increasing Z' or Z, this implies that there is only a peak.

In Figure 4, we plot the variations of Josephson critical current I_C for the heavy and light holes with Z (Z') at different Z' (Z) in the A alignment. It is found that although there are the features which are the same as those in Figure 3, the values of the critical Josephson currents I_C with the increase of Z or Z' are a little different, which can be also ascribed to the same reason as in the explanation of the same and different properties between Figures 1 and 2. Here, the differences of the results between the heavy and light holes in Figure 4, together with Figures 1–3, can be all explained by the fact that there are the different mismatches in the effective mass and Fermi velocity between the FS and SC for the two kinds of holes.

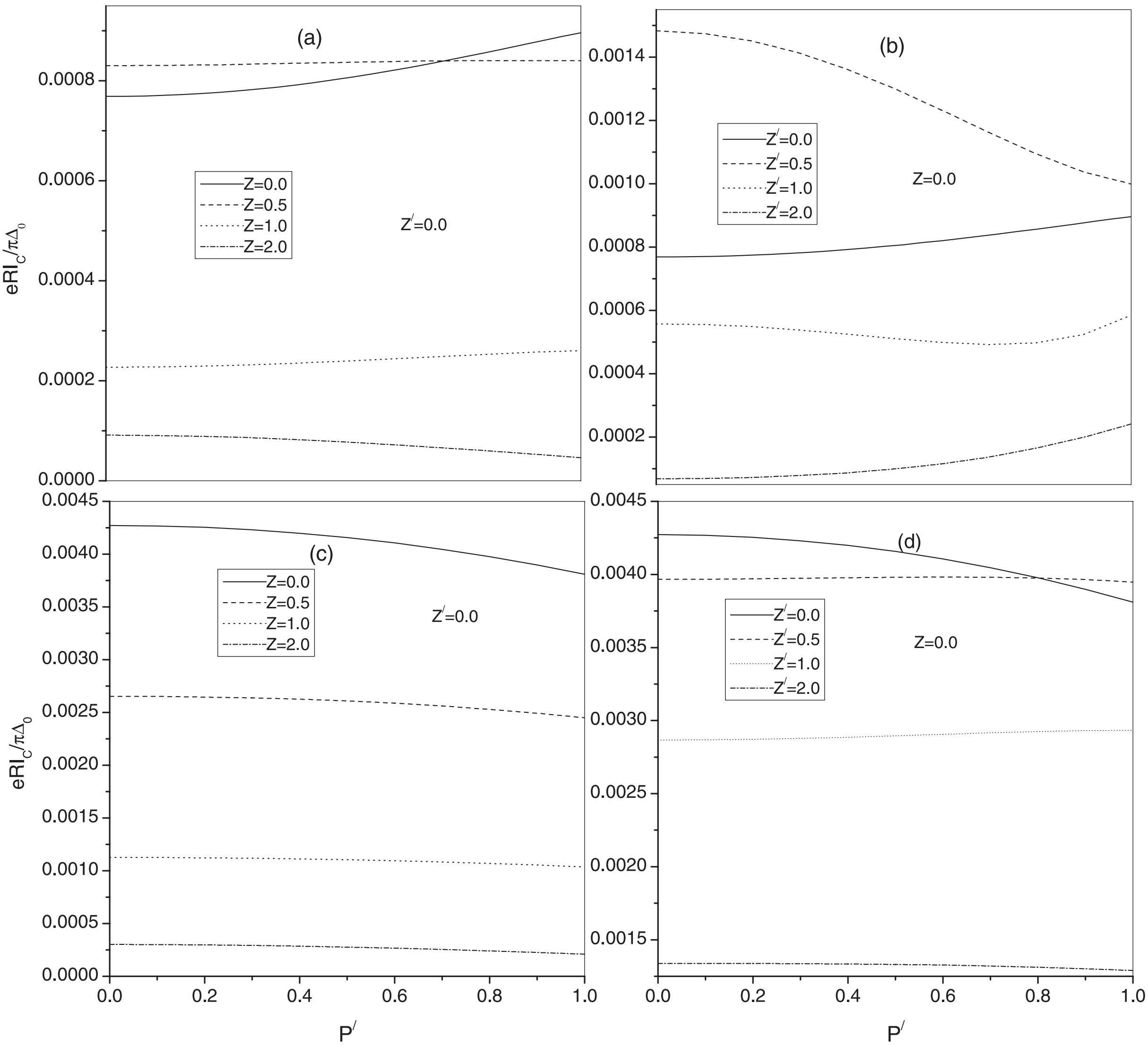

Fig. 1. Dependence of the normalized critical current I_C on P in the F alignment at different scattering potential strengths: Z (a) and Z' (b) for the heavy holes; Z (c) and Z' (d) for for the light. The parameters $E_F = 100.0$ meV, $\Delta_0 = 1.4$ meV, $k_B T = 0.05\Delta_0$, $a = 40/k_F^{SC}$, $b = 20/k_F^{SC}$, $m_e = 1.0$, and $m_p = 0.45m_e$ for the heavy hole and $0.08m_e$ for the light hole in the FS and SM.

Microscopically, the transfer of Cooper pairs through the FS occurs via Andreev reflections [16,25]. A holelike excitation in FS with energy lower than the superconducting energy Δ, can not enter into the SC. It is reflected at the FS/SC interface as an electron and then reflected back as a hole at the opposite SC/FS interface, in the meantime, it undergoes twice normal reflections in the FS/SM and SM/FS interfaces. The constructive interferences of the holelike and electronlike excitations give rise to Andreev bound state in FS and SM, which carry the supercurrent. However, in the FS, the Andreev reflection is affected by the spin splitting of the spin band as the Andreev reflections reverse the spin of the quasiparticles, this implies that the exchange energy is gained or lost by a quasiparticle Andreev-reflected at the FS/SC interface. As a result, the spin polarization in the FS modulates the Josephson current as in Figures 1 and 2. Obviously, the relative orientations of the FS's strongly determine the Josephson current as shown in Figures 1 and 2, since in the F alignment of the magnetizations of the two FS's, the spin-up (spin-down) holes tunneling into the SM through the left FS/SM interface and tunneling out of the SM through the right SM/FS interface do not change their wave vectors, however, in the A alignment, the situation is quite different, i.e., after tunneling into the right FS, the vectors of the holes are varied. In addition, the reflections including the Andreev reflection at the SC/FS (FS/SC) and FS/SM (SM/FS) interfaces are strongly dependent on the Z and Z', respectively, therefore, as shown in Figures 1–4, Z and Z' have different effects on the Josephson current. Similarly, the differences of the results for the Josephson current between the heavy and light holes can

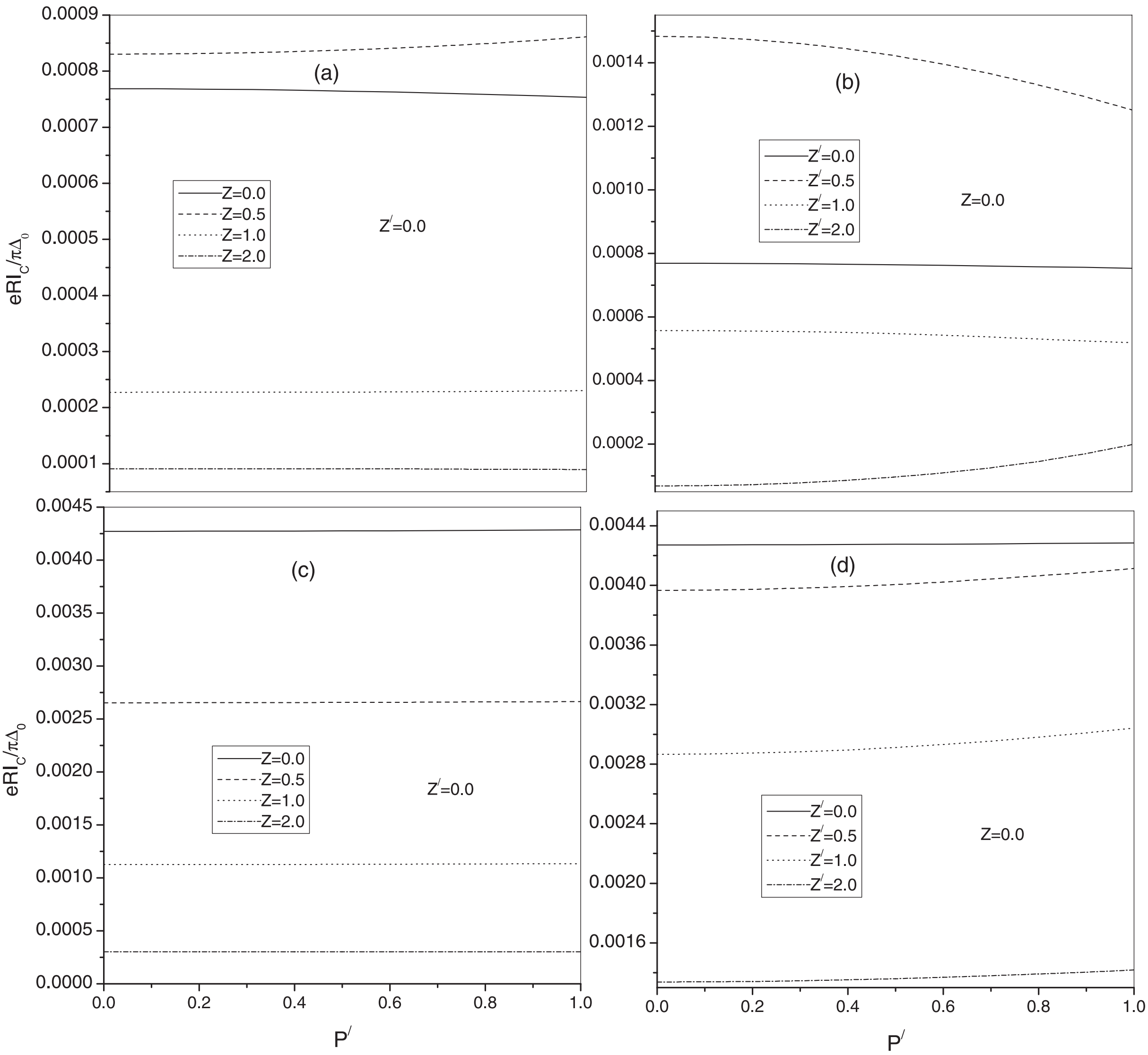

Fig. 2. The same dependence as in Figure 1 in the case of the A alignment.

be explained by the fact that the spin polarization and $Z\,(Z')$ have different influences on the Josephson current due to the different mismatches in the effective masses and Fermi velocity between the FS and SC for the two kinds of holes.

In what follows, a robust approach to measuring the spin polarizations P for the heavy and light holes is presented here in the case approximate to the metallic contact, which can be produced experimentally as has been fabricated by Bareden et al. [12]. In the F alignment, during the region where the spin polarizations are generally big for the FS, the variations of Josephson critical currents I_{hF} and I_{lF} for the heavy and light holes with P'_h and P'_l as shown in Figure 1 can be described by approximately linear relations with slopes ζ, i.e., $I_{hF} = \zeta_{hF}P'_h + I_{hF0}$ and $I_{lF} = \zeta_{lF}P'_l + I_{lF0}$, respectively, where $\zeta_{hF} = 1.273 \times 10^{-4}\pi\Delta_0/eR$, $\zeta_{lF} = -4.621 \times 10^{-4}\pi\Delta_0/eR$, $I_{hF0} = 7.689 \times 10^{-4}\pi\Delta_0/eR$, and $I_{lF0} = 4.272 \times 10^{-3}\pi\Delta_0/eR$. Similarly, in the A alignment shown in Figure 2, $I_{hA} = \zeta_{hA}P'_h + I_{hA0}$ and $I_{lA} = \zeta_{lA}P'_l + I_{lA0}$ with $\zeta_{hA} = -0.1549 \times 10^{-4}\pi\Delta_0/eR$, $\zeta_{lA} = 0.1275^{-4}\pi\Delta_0/eR$, $I_{hA0} = 7.689\times 10^{-4}\pi\Delta_0/eR$, and $I_{lA0} = 4.272 \times 10^{-3}\pi\Delta_0/eR$. For either the F or A magnetic alignments, the total current is the sum of those for the heavy and light holes, in which the weights are determined by the respective densities. Provided that I_F and I_A from experiments are obtained, we can extract P'_l and P'_h from the following two equations

$$I_F = n_h/(n_h + n_l)I_{hF} + n_l/(n_h + n_l)I_{lF}, \tag{9}$$

$$I_A = n_h/(n_h + n_l)I_{hA} + n_l/(n_h + n_l)I_{lA}, \tag{10}$$

where $n_{h(l)} \sim (m_p)^{\frac{3}{2}}$ is the density of heavy (light) holes in valence subband of the FS. Based on P'_h and P'_l, one can obtain the spin polarizations P_h and P_l for the heavy and light holes by means of the formula $P = P'\Delta_0/E_F$.

Next the appealing and possible applications are discussed. In the above calculations, there may be some

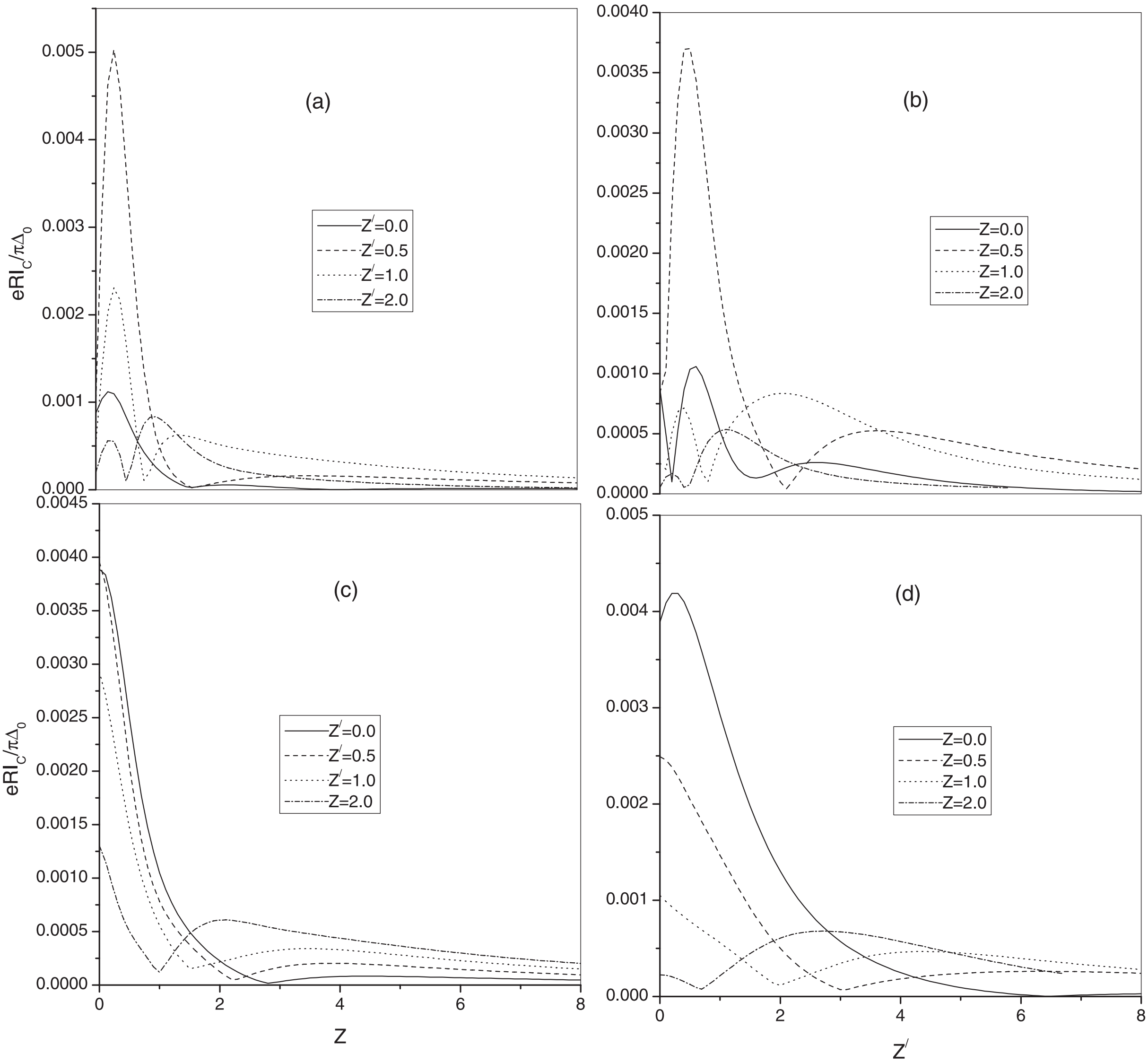

Fig. 3. Dependence of I_C on Z and Z' at $P = 0.9$ with the same situations as in Figure 1.

consequence on spin correlation when the transport takes place on such lengths of a and b. In fact, the Fermi energy E_F^{SC} can be much bigger than that chosen in the work. For the simplicity, the results are only given for the E_F approaching that in the FS and the effects on spin correlation is not considered, to have an insight into the effect of the difference of mass between the FS and SC. According to the calculations, for the bigger Fermi energy E_F in the SC, although the k_F^{SC} is much bigger than k_F^{FS} when the difference of the band widths between the FS and SC should be considered, which is different from that for the smaller Fermi energy E_F in the SC, there is no significant change of the conclusions. In real experiments, one can choose a superconductor with bigger Fermi energy such as Ga and Al, $Ga_{0.95}Mn_{0.05}As$ with high P and GaAs. A single junction composed of GaMnAs and Ga has been fabricated in reference [12].

Lastly, I want to briefly discuss the effects of the phase on the current which characterize the Josephson coupling across a Josephson junction. As in the SC/FM/SC junctions references [25], the Josephson current in our model changes sign with the phase shift ϕ, which can be understood by equations (A4–A13). However, the situation is different from that in SC/FM/SC junctions. If the junction is the 0 or π state or the transition from the 0 to π state is determined by both the magnetic alignments and the kinds of the carriers, namely, the heavy or light holes.

4 Summary

We apply a general expression for dc Josephson current to investigate the Josephson effect of SC/FS/SM/FS/SC junctions, in which the spin polarization in the FS, mismatches in the effective mass and Fermi velocity between the FS and SC, together with strengths of potential scattering at the interfaces are considered. It is found that the critical Josephson current I_C in the junction is strongly

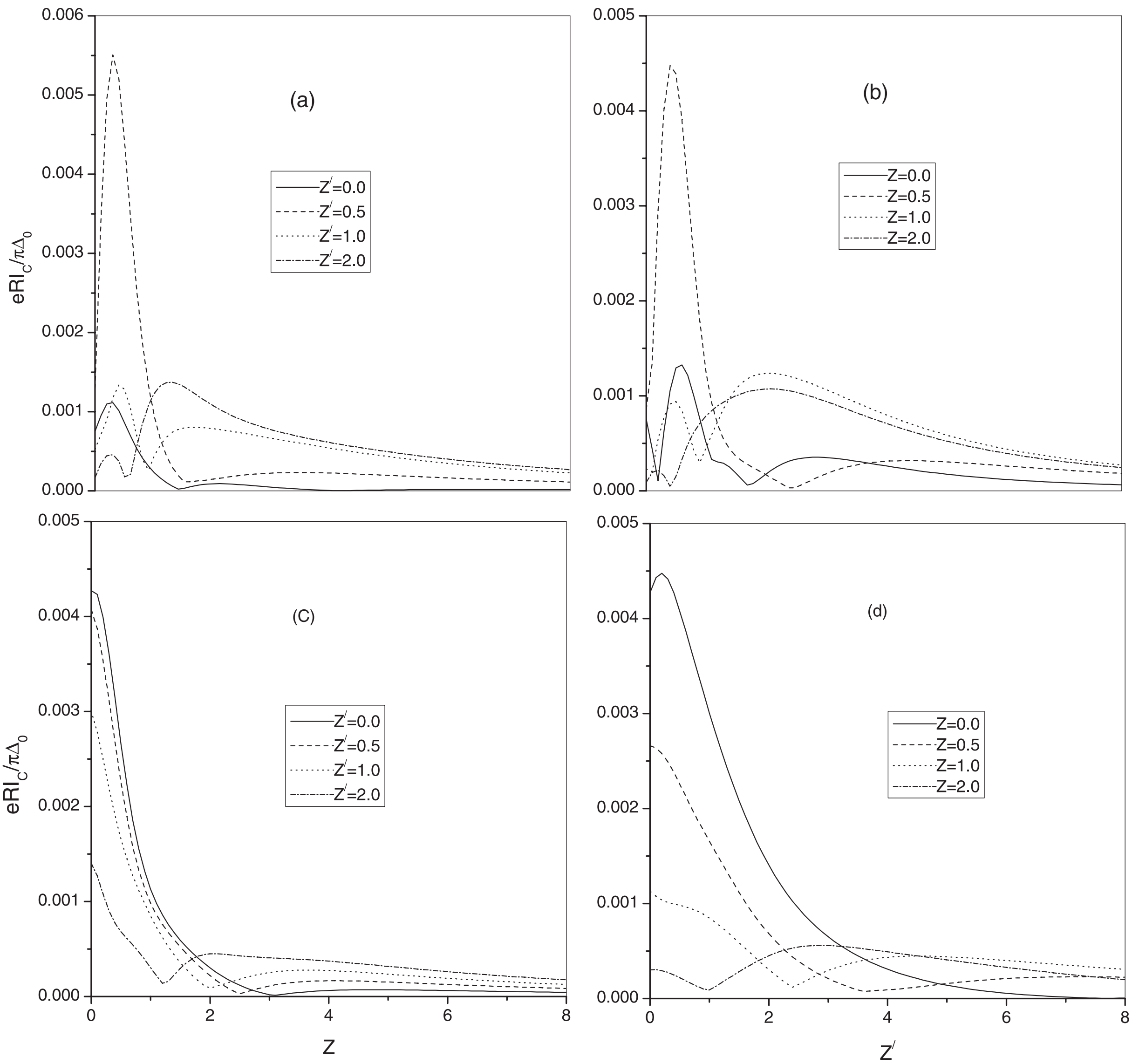

Fig. 4. Dependence of I_C on Z and Z' at $P = 0.9$ with the same situations as in Figure 2.

dependent on not only the kinds of holes (the heavy or light ones) in the FS and strengths of potential scattering at the interfaces but also the relative orientations of the effective exchange field **h** of the two FS layers. In addition, a robust approach to measuring the spin polarizations for the heavy and light holes is proposed. Here, the two dimensionless parameters Z and Z' and the whole approach in the model show strong similarities to the theory developed by Blonder et al. [33]. It is a comprehensive theory to evaluate the conductance spectra of superconductor/normal metal junctions with arbitrary interfacial scattering strength, bridging the gap between metallic contacts in tunnel junctions. In our model, the metallic metal is replaced by the FS, so the different kind of holes (the heavy and light) are considered, i.e., different mismatch in the effective mass and Fermi velocity are included.

Furthermore, it is expected that theoretical results obtained will be confirmed in the future experiments. The research of the junctions can provide new opportunities for the research of the SC and FS systems, which could not only be used for reliable spectroscopy of Josephson current and bring about promising interest for the further enhancement of the efficiency in magnetic sensors and memories but also be helpful to have an insight into the physical properties of the heavy and light holes in the FS.

It is pointed that, the step function approximation is used for the pair potential [12,25], but in the case of low interfacial transparency, two kinds of holes, and/or thin interlayers, our results will not be altered significantly. In that case, the depletion of the pair potential in the superconductors is negligible. Characteristic proximity effects at transparent FS interfaces have to be studied by a self-consistent numerical treatment [21,26]. In addition, as commonly evidenced in other theoretical results [12,25], the barrier transparency of involved interfaces plays an important role in our model, however the role is closely connected with not only the magnetic configurations but also the kinds of the holes and Z and Z' have different influences on the critical Josephson current, as shown in Figures 1–4, which is natural. Besides, as is pointed out by reference [30], the mean free path for elastic scattering of the carriers is much smaller than that for inelastic scattering from the impurities also magnetic in the structures, which indicates that the carriers undergo some elastic scattering and the inelastic scattering is expected to be unimportant. We also adopt other various simplifying approximations such as δ-function model for interface scattering, no spin-flip process, etc., however they are nonessential, made for the sake of analytical simplicity, and may be improved by the future numerical treatment with available experimental data. Inclusion of these effects would be necessary for a complete theory, which merits further study.

This work was supported in part by the National Science Foundation of China under Grant No. 10347118 and Natural Science Foundation of Jiangsu Education Department of China under Grant No. 2004102TSJB141.

Appendix: Expressions for reflection and transmission coefficients in the P alignment

$$a_\sigma = A_1/A_0, \tag{A.1}$$

with

$$A_0 = \begin{vmatrix} \alpha_{e11} & \alpha_{e12} & \alpha_{e13} & \alpha_{e14} \\ \alpha_{e21} & \alpha_{e22} & \alpha_{e23} & \alpha_{e24} \\ \alpha_{h11} & \alpha_{h12} & \alpha_{h13} & \alpha_{h14} \\ \alpha_{h21} & \alpha_{h22} & \alpha_{h23} & \alpha_{h24} \end{vmatrix}, \tag{A.2}$$

$$A_1 = \begin{vmatrix} \alpha_{e10} & \alpha_{e12} & \alpha_{e13} & \alpha_{e14} \\ \alpha_{e20} & \alpha_{e22} & \alpha_{e23} & \alpha_{e24} \\ \alpha_{h10} & \alpha_{h12} & \alpha_{h13} & \alpha_{h14} \\ \alpha_{h20} & \alpha_{h22} & \alpha_{h23} & \alpha_{h24} \end{vmatrix}, \tag{A.3}$$

where

$$\begin{aligned}\alpha_{e10} &= u(q'^+ + Z' + q_\sigma^{L+})(q_\sigma^{L+} + Z \\ &\quad + \chi k^+)e^{-i[(k^+ - q'^+)a/2 + (k^+ - q_\sigma^{L+})b - \phi]} \\ &\quad + u(q'^+ + Z' - q_\sigma^{L+})(q_\sigma^{L+} - Z \\ &\quad - \chi k^+)e^{-i[(k^+ - q'^+ a/2 + (k^+ + q_\sigma^{L+})b - \phi]},\end{aligned} \tag{A.4}$$

$$\begin{aligned}\alpha_{e20} &= u(q'^+ - Z' - q_\sigma^{L+})(q_\sigma^{L+} + Z \\ &\quad + \chi k^+)e^{-i[(k^+ + q'^+)a/2 + (k^+ - q_\sigma^{L+})b - \phi]} \\ &\quad + u(q'^+ - Z' + q_\sigma^{L+})(q_\sigma^{L+} - Z \\ &\quad - \chi k^+)e^{-i[(k^+ + q'^+)a/2 + (k^+ + q_\sigma^{L+})b - \phi]},\end{aligned} \tag{A.5}$$

$$\begin{aligned}\alpha_{e11} &= -v(q'^+ + Z' + q_\sigma^{L+})(q_\sigma^{L+} + Z \\ &\quad + \chi k^-)e^{-i[(k^- - q'^+)a/2 + (k^+ - q_\sigma^{L+})b - \phi]} \\ &\quad - v(q'^+ + Z' - q_\sigma^{L+})(q_\sigma^{L+} - Z \\ &\quad - \chi k^-)e^{-i[(k^+ - q'^+ a/2 + (k^+ + q_\sigma^{L+})b - \phi]},\end{aligned} \tag{A.6}$$

$$\begin{aligned}\alpha_{e21} &= -v(q'^+ - Z' - q_\sigma^{L+})(q_\sigma^{L+} + Z \\ &\quad + \chi k^-)e^{-i[(k^- + q'^+)a/2 + (k^+ - q_\sigma^{L+})b - \phi]} \\ &\quad - v(q'^+ - Z' + \chi q_\sigma^{L+})(q_\sigma^{L+} - Z \\ &\quad - \chi k^-)e^{-i[(k^- + q')a/2 + (k^- + q_\sigma^{L+})b - \phi]},\end{aligned} \tag{A.7}$$

$$\begin{aligned}\alpha_{e12} &= -u(q'^+ + Z' + q_\sigma^{L+})(q_\sigma^{L+} + Z \\ &\quad - \chi k^+)e^{i[(k^- + q'^+)a/2 + (k^+ + q_\sigma^{L+})b + \phi]} \\ &\quad - u(q'^+ + Z' - q_\sigma^{L+})(q_\sigma^{L+} - Z \\ &\quad + \chi k^+)e^{i[(k^+ + q'^+)a/2 + (k^+ - q_\sigma^{L+})b + \phi]},\end{aligned} \tag{A.8}$$

$$\begin{aligned}\alpha_{e22} &= -u(q'^+ - Z' - q_\sigma^{L+})(q_\sigma^{L+} + Z \\ &\quad - \chi k^+)e^{i[(k^+ - q'^+)a/2 + (k^+ + q_\sigma^{L+})b + \phi]} \\ &\quad - u(q'^+ - Z' + q_\sigma^{L+})(q_\sigma^{L+} - Z \\ &\quad + \chi k^+)e^{i[(k^+ - q'^+)a/2 + (k^+ - q_\sigma^{L+})b + \phi]},\end{aligned} \tag{A.9}$$

$$\begin{aligned}\alpha_{e13} &= u(q'^+ - Z' + q_\sigma^{R+})(q_\sigma^{R+} - Z \\ &\quad + \chi k^+)e^{i[(k^+ - q'^+)a/2 + (k^+ - q_\sigma^{R+})b]} \\ &\quad + u(q'^+ - Z' - q_\sigma^{R+})(q_\sigma^{R+} + Z \\ &\quad - \chi k^+)e^{i[(k^+ - q'^+)a/2 + (k^+ + q_\sigma^{R+})b]},\end{aligned} \tag{A.10}$$

$$\begin{aligned}\alpha_{e23} &= u(q'^+ + Z' - q_\sigma^{R+})(q_\sigma^{R+} - Z \\ &\quad + \chi k^+)e^{i[(k^+ + q'^+)a/2 + (k^+ - q_\sigma^{R+})b]} \\ &\quad + (q'^+ + Z' + q_\sigma^{R+})(q_\sigma^{R+} + Z \\ &\quad - \chi k^+)e^{i[(k^+ + q'^+)a/2 + (k^+ + q_\sigma^{R+})b]},\end{aligned} \tag{A.11}$$

$$\begin{aligned}\alpha_{e14} &= v(q'^+ - Z' + q_\sigma^{R+})(q_\sigma^{R+} - Z \\ &\quad - \chi k^-)e^{-i[(k^- + q'^+)a/2 + (k^- + q_\sigma^{R+})b]} \\ &\quad + v(q'^+ - Z' - pq_\sigma^{R+})(q_\sigma^{R+} + Z \\ &\quad + \chi k^-)e^{-i[(k^+ + q'^+)a/2 + (k^+ - q_\sigma^{R+})b]},\end{aligned} \tag{A.12}$$

$$\begin{aligned}\alpha_{e24} &= v(q'^+ + Z' - q_\sigma^{R+})(q_\sigma^{R+} - Z \\ &\quad - \chi k^-)e^{-i[(k^+ - q'^+)a/2 + (k^+ + q_\sigma^{R+})b]} \\ &\quad + v(q'^+ + Z' + q_\sigma^{R+})(q_\sigma^{R+} + Z \\ &\quad + \chi k^-)e^{-i[(k^- - q'^+)a/2 + (k_h^- - q_\sigma^{R+})b]},\end{aligned} \tag{A.13}$$

and the terms from α_{h10} to α_{h24} can be obtained through equations (A4–A13) with $k^+ \to k^-$, $q_\sigma^{L(R)+} \to q_\sigma^{L(R)-}$, $q'^+ \to q'^-$, and $\phi \to -\phi$.

References

1. G. Prinz, Phys. Today **48**, 58 (1995)
2. L.J. Sham, J. Phys: Condens. Matter **5**, 51 (1993); D.P. DiVincenzo, Science **270**, 255 (1995); J. Fabian, S. Das Sarma, Phys. Rev. Lett. **81**, 5624 (1998); J. Fabian, S. Das Sarma, J. Vac. Sci. Technol. B **17**, 1708 (1999); J. Fabian, S. Das Sarma, J. Appl. Phys. **85**, 5705 (1999)
3. S. Datta, B. Das, Appl. Phys. Lett. **56**, 665 (1990)
4. J.M. Kikkawa, D.D. Awschalom, Phys. Rev. Lett. **80**, 4313 (1998); J.M. Kikkawa, D.D. Awschalom, Nature (Lodon) **397**, 139 (1999); I. Malajovich, I.J. Berry, N. Samarth, D.D. Awschalom, Nature (London) **411**, 770 (2001); D.D. Awschalom, J.M. Kikkawa, Phys. Today **52**, 33 (1999)
5. M. Johnson, Phys. Rev. B **58**, 9635 (1998)
6. H. Ohno, in *Semiconductor Spintronics and Quantum Computation*, edited by D.D. Awschalom, N. Samarth, D. Loss (Springer, New Yok, 2002), p. 1
7. H. Ohno, Science **281** (1991); J. Magn. Magn. Matter. **200**, 110 (1999)
8. T. Dietl, H. Ohno, F. Matsukura, J. Cibert, D. Ferrand, Science **287**, 019 (2000)
9. J. Konig, H.-H. Lin, A.H. MacDonald, Phys. Rev. Lett. **84**, 5682 (2000); J. Konig, T. Jungwirth, A.H. MacDonald, Phys. Rev. B **64**, 184423 (2001)
10. K.C. Ku et al., Appl. Phys. Lett. **82**, 2302 (2003)
11. Y.C. Tao, J.G. Hu, H. Liu, J. Appl. Phys. **96**, 498 (2004); Y.C. Taon, J.G. Hu, Phys. Rev. B **72**, 165329 (2005)
12. J.G. Braden, J.S. Parker, P. Xiong, Phys. Rev. Lett. **91**, 056602 (2003)
13. A.D. Giddings, M.N. Khalid, T. Jungwirth, J. Wunderlich, S. Yasin, R.P. Campion, K.W. Edmonds, J. Sinova, K. Ito, K.-Y. Wang, D. Williams, B.L. Gallagher, C.T. Foxon, Phys. Rev. Lett. **94**, 127202 (2005); M. Tanaka, Y. Higo, Phys. Rev. Lett. **87**, 026602 (2001)
14. B.D. Josephson, Phys. Lett. **1**, 251 (1962)
15. V.V. Ryazanov, V.A. Oboznov, A.Yu. Rusanov, A.V. Veretennikov, A.A. Golubov, J. Aarts, Phys. Rev. Lett. **86**, 2427 (2001)
16. T. Kontos, M. Aprili, J. Lesueur, X. Grison, Phys. Rev. Lett **86**, 304 (2001); T. Kontos, M. Aprili, J. Lesueur, F. Genêt, B. Stephanidis, R. Boursier, Phys. Rev. Lett. **89**, 137007 (2002)
17. O. Bourgeois, P. Gandit, J. Lesueur, A. Sulpice, X. Grison, J. Chaussy, Eur. Phys. J. B **21**, 75 (2001)
18. M. Fogelström, Phys. Rev. B **62**, 11812 (2000)
19. F.S. Bergeret, A.F. Volkov, K.B. Efetov, Phys. Rev. Lett. **86**, 3140 (2001); F.S. Bergeret, A.F. Volkov, K.B. Efetov, Phys. Rev. B **65**, 134505 (2002); F.S. Betrgert, A.F. Volkov, K.B. Efetov, Rev. Mod. Phys. **77**, 1321 (2005)
20. V.N. Krivoruchko, E.A. Koshina, Phys. Rev. B **64**, 172511 (2001)
21. N.M. Chtchelkatchev, W. Belzig, Yu.V. Nazarov, C. Bruder, Pis'ma Zh. Éksp. Teor. Fiz. **74**, 357 (2001) [JETP Lett. **74**, 323 (2001)]; M. Zareyan, W. Belzig, Yu.V. Nazarov, Phys. Rev. Lett. **86**, 308 (2001)
22. A.A. Golubov, M.Yu. Kupriyanov, Ya.V. Fominov, Pis'ma Zh. Éksp. Teor. Fiz. **75**, 709 (2002) [JETP Lett. **75**, 588 (2002)]; A.A. Golubov, M.Yu. Kupriyanov, E. Il′ichev, Rev. Mod. Phys. **76**, 411 (2004)
23. Yu.S. Barash, I.V. Bobkova, T. Kopp, Phys. Rev. B **66**, 140503 (2003)
24. A.Yu. Zyuzin, B. Spivak, M. Hruška, Europhys. Lett. **62**, 97 (2003)
25. Z. Radović, L. Dobrosavljević-Grujić, B. Vujičić, Phys. Rev. B **63**, 214512 (2001); M. Božović, Z. Radović, Phys. Rev. B **66**, 134524 (2002); Z. Radović, N. Lazarides, N. Flytzanis, Phys. Rev. B **68**, 014501 (2003)
26. K. Halterman, O.T. Valls, Phys. Rev. B **65**, 014509 (2002)
27. I. Baladie, A. Buzdin, Phys. Rev. B **64**, 224514 (2001)
28. J.S. Jiang, D. Davidović, D.H. Reich, C.L. Chien, Phys. Rev. Lett. **74**, 314 (1995); Y. Obi, M. Ikebe, T. Kubo, H. Fujimori, Physica C **317–318**, 149 (1999)
29. A.I. Buzdin, Rev. Mod. Phys. **77**, 935 (2005)
30. W.M. van Huffelen, T.M. Klapwijk, D.R. Heslinga, M.J. de Boer, N. van der Post, Phys. Rev. B **47**, 5170 (1993)
31. A. Furusaki, M. Tsukada, Solid State Commun. **78**, 299 (1991)
32. T. Hayashi, M. Tanaka, A. Asamitsu, J. Appl. Phys. **87**, 4673 (2000)
33. G.E. Blonder, M. Tinham, T.M. Klapwijk, Phys. Rev. B **25**, 4515 (1982)